A flexible approach to assessing synchroneity of past events using Bayesian reconstructions of sedimentation history

A.C. Parnell [a] J. Haslett [a] J.R.M. Allen [b] C.E. Buck [c]
B. Huntley [b]

[a] *Department of Statistics, Trinity College Dublin*

[b] *School of Biological and Biomedical Sciences, Durham University*

[c] *Department of Probability and Statistics, University of Sheffield*

Abstract

The dating of depths in two or more cores is frequently followed by a study of the synchroneity or otherwise of events reflected in the cores. The difficulties most frequently encountered are: (a) determining precisely the depths associated with the events; and (b) determining the ages associated with the depths. There has been much progress in recent years in developing tools for the study of uncertainties in establishing chronologies. This has not yet been matched by similar progress in modelling event/depth relationships. This paper proposes a simple and flexible approach, showing how uncertain events can be married to uncertain chronologies.

Difficulties in studying event/depth/age relationships typically involve a confounding of two different problems. First, what exactly do we mean by an 'event' - a point in history, a single depth in the core corresponding to a single time, or a depth/time range? Sometimes 'event' is in fact a shorthand for a space-time process. Do the data reflect more than one type of event/process? This can reflect vagueness in definition. Second, what are the sources and implications of the uncertainties?

Here we illustrate the issues involved by examination of several features seen in north European Holocene pollen records. The *Alnus* rise is regarded as a diachronous early Holocene event; in contrast the *Ulmus* decline is widely seen as a near synchronous event in the mid-Holocene. The third feature we examine is the interval between the *Ulmus* decline and the first occurrence of Cerealia-type pollen. The evidence for these events lies in cores of lake sediment from which are determined: (a) the proportions of pollen at many depths; and (b) radiocarbon age estimates from, usually, fewer depths. For this illustration we focus on six sites.

We draw attention to a new and flexible method (implemented in the free `R` software package `Bchron`; Haslett and Parnell, 2008) for the establishment of the uncertainties surrounding the dating of samples in such cores. We illustrate its flexibility by assessing the synchroneity of past events.

Preprint submitted to Elsevier *2 July 2008*

Key words: contemporaneity, synchroneity, Bayesian modelling, *Alnus* rise, *Ulmus* decline

1 Introduction

An issue of considerable importance to our understanding of Quaternary palaeoenvironmental history is that of establishing synchroneity in events recognised in two or more stratigraphic records. Where the event appears asynchronous, an important second issue is that of establishing the extent of the asynchrony (see e.g. Davis, 1983; Birks, 1989; Alley et al., 1997; Haas et al., 1998; Bennett and Fuller, 2002; Blaauw et al., 2007). A common challenge is the uncertainty in establishing the age of the event in each of those records, as well as the identification of the event itself. This paper proposes a new and flexible approach to modelling such uncertainties and thus to the drawing of appropriately qualified scientific conclusions.

We illustrate this new approach using three events apparent in palynological data in northern Europe from six sites at each of which there is partial ^{14}C dating information. These events are: (1) the early- to mid-Holocene increase in abundance of *Alnus* (alder) pollen ('the alder rise'); (2) the mid-Holocene decline in abundance of *Ulmus* (elm) pollen ('the elm decline'); and (3) the first mid- to late-Holocene occurrence of Cerealia-type pollen. We assess the degree of synchroneity across a number of sites of the first two events, and also compare the intervals between the last two events at the same sites. We suggest, however, that the overall approach is of wide relevance.

Notwithstanding its central importance in many aspects of Quaternary science, the problems associated with making such assessments of synchroneity have received remarkably little attention. For example, while a web search readily finds dozens of papers using the term "degree of synchroneity/synchronicity of an event" in the context of the Holocene, neither the terms synchroneity nor event are typically defined. Yet precise formal definitions are vital for the discussion of uncertainty. As discussed in this paper, we define an 'event' to be a unique point in time at a precise location in space. We study the time differences between pairs of such events each measured with uncertainty. Technically these are measures of the degree of diachroneity, in the presence of statistical noise. Typically events, as so defined, reflect unobserved space-time processes, such as the *Ulmus* decline, and study focusses on spatial structure in the degree of diachroneity.

Email address: `Andrew.Parnell@tcd.ie` (A.C. Parnell).

From a much wider spatio-temporal perspective, the *Ulmus* decline across NW Europe is itself an 'event'; indeed this is the sense in which we use it in the previous paragraph. It would be pedantic to insist always on separate terms for both the 'unique in time and space' event and the 'spatio-temporal process' event. Thus in general discussion below we will sometimes use the term in both senses, leaving the context to make it clear to the reader. Nevertheless, in our discussion of synchroneity in the presence of uncertainty, events are as defined above and as elaborated and illustrated below.

We identify three general aspects of the problem. First, there are problems associated with characterising the event itself, and hence in determining the depth at which the event occurred in a given stratigraphic sequence. If we are to associate an event with a point in history, a single depth in the core, what are the implications? Closely related to this is the establishment of the uncertainty about this depth, given the data available. Finally, there are challenges in assigning an age to this depth, with an associated statement of uncertainty. These latter are issues of statistical inference.

The structure of the paper is as follows. In Section 2 we discuss approaches to event definition, chronology modelling and synchroneity. Section 3 presents the data and proposes depth intervals for the events. Section 4 presents an illustration of various approaches applied to six selected sites around north-western Europe. Finally, in Section 5, we discuss the potential of the new approach with further illustrations.

2 Methods

We discuss here the identification of events in terms of depth and the subsequent estimation of their associated ages, with uncertainty on both. Our simplest proposals in respect of depth uncertainty are very easy to implement and can be regarded as typically adequate approximations to a formal statistical analysis. In respect of age estimation, especially for depths where ^{14}C age information is not available, the implementation requires specialist software (`Bchron`), although the concepts are simple. We refer the reader to the Appendix for instructions as to how to access the software. These are all discussed in the two sections following. In a third section, we discuss Monte Carlo methods for the amalgamation of events, ages and their associated uncertainties into a framework for the study of synchroneity. Such methods arise naturally in a Bayesian context which provides the basis for the flexibility of the approaches offered in this paper. We return in the final section to the term 'synchroneity'. Readers whose primary interest is in our findings may wish to skim this section at first reading.

2.1 Events

It is necessary at the outset to distinguish between the definition of the term 'event' and the operational mechanics of its uncertain location in the core, given data (here pollen percentages). Events are not observable; they are latent and observed through, but not defined by, noisy data. An 'event' is thus a theoretical construct. To some this distinction will seem to be over-formal given the uncertainties of measurement. Nevertheless it is such confounding that lies at the heart of much of the conflict that can sometimes be apparent in scientific findings (e.g. the Younger Dryas: Turney et al., 2007; Boes and Fagel, 2008). If we cannot say what an event is we cannot always usefully discuss with others the uncertainty in the unique depth and age that we propose to associate with it.

For example, Smith and Pilcher (1973) proposed the term 'rational limit' for an event as reflected by pollen data, defining this as the time of the first rapid increase in pollen taxon abundance. This proposal has been widely adopted, especially by authors of isochrone maps that seek to portray the timing of the 'arrival' of a taxon across some geographical region (e.g. Birks, 1989; Davis, 1976). Smith and Pilcher (1973) also proposed the term 'empirical limit' for the time after which a pollen taxon is consistently present. As Watts (1973) noted, however, a limit defined in this way is very sensitive to the relative abundance of the taxon in question, the number of pollen grains counted and the depth resolution of pollen counts. Such definitions leave considerable scope for uncertainty as to the precise location in a pollen core of the event.

Problems of identifying the depth of an event arise because of stochastic noise in the determination of the event and in the observed data. Such noise can arise from various sources, although these essentially fall into two categories. First, the pollen data values themselves are noisy. Such noise arises partly from inherent randomness in collecting, identifying and counting the number of pollen grains in a sample. It can also result from temporal, especially inter-annual, variations in pollen production by species that do not reflect changes in vegetation composition but result from differential sensitivity of flowering and pollen production to short-term climatic variability amongst species (Autio and Hicks, 2004).

Second, noise can relate to the action of various agencies of vegetation disturbance that operate at local as opposed to regional or global scales (e.g. wildfire, damage by extreme weather events, intense herbivory, shifting cultivation) but that can result in changes in the pollen record that mimic regionally or globally recognisable events. Thus a local event, even if clearly observed in the pollen record, can itself be a type of noise. But this can only be seen in a wider spatio-temporal context, and even then may not always be clearly seen.

Distinguishing regional and global events is thus a matter of definition; if the process under study is global, then events reflecting regional scale processes may not be events.

Considering an event at a point in space, we see that it may take one of two general forms. Most commonly, it will be a transition (often but not necessarily rapid) from one stable palaeoenvironmental state to another, characterised by stability over a period of time (or depth); see for example Figure 1. Examples include: a change in the composition of the micro-fossil assemblage in a sediment core; a relatively rapid change in the value of some physical palaeoenvironmental indicator such as the δ^{18}O value of ice or of a speleothem. Less often, the event will be a short-lived excursion from the longer-term mean state of some component(s) of the system; for example, the deposition of a tephra layer within a sediment sequence.

Here we focus upon transition events. In Figure 1 the observed palaeoenvironmental proxy $\hat{p}$, given as a proportion, reflects a conceptual unobserved value p which rises from p_{min} to a level p_{max}; conversely there may be a decline. We can formalize this via a function $g(d)$ of depth; thus $p(d) = p_{min}+g(d)(p_{max}-p_{min})$, where $g(d)$ is a sigmoid function rising from $g(d_0) = 0$ to $g(d_1) = 1$ (conversely declining). Generally $g(d)$ and aspects of it such as d_{event} are unobserved, although noisy data are available.

The identification of an event with a single point on such a curve is an entirely theoretical exercise. The definition we shall take here is that d_{event} is the midpoint; that is, that depth d_{mid} at which $g(d) = \frac{1}{2}$. If $g(d)$ is symmetric (strictly, in the above context, rotationally symmetric) then this is also the point at which $g(d)$ is steepest; $d_{event} = d_{steep}$. Note that it cannot generally be defined as $d_{event} = \frac{1}{2}(d_0 + d_1)$, as d_0 and d_1 are $\pm\infty$ in many natural models for $g(d)$ (e.g. the logistic model). Other definitions of 'event' are possible. The start or end of an event with associated unique depths d_{start} or d_{end} could be points of interest, providing they can be defined in terms of a suitable curve; note that the use of d_{mid} avoids this necessity. Similarly events could in principle be defined in terms of an interval, with profound implications for the concept of synchroneity (see, for example, McColl, 2008, Ch.5).

The precision with which d_{event} is determined is a separate issue of statistical inference. It is largely dependent on the sampling interval relative to the rapidity of the event and to the size of the samples, itself relating to the random noise in the proxy signal. Typically, a transition event may occur between two successive samples; see Figure 1. Widespread present practice is simple but crude. It may be characterised as: (i) identify depths d_{min} and d_{max} above and below the event; (ii) define $d_{event} = \frac{1}{2}(d_{max} + d_{min})$; and (iii) ignore depth uncertainty. Given the dating uncertainty, this may often suffice. Here we make the more cautious assumption only that d_{event} is equally likely to be anywhere within the interval (d_{min}, d_{max}). In more formal Bayesian terms, we shall say that the distribution of d_{event}, in the light of a pollen diagram, is Uniform on the interval (d_{min}, d_{max}). For sites where multiple intervals are appropriate, we define $(d^{(1)}_{min}, d^{(1)}_{max})$, $(d^{(2)}_{min}, d^{(2)}_{max})$, etc, and allow d_{event} to be Uniform over both ranges. For the sites we have chosen, identification of these 'by eye' should be entirely sufficient. It is possible to take more formal approaches to statistical inference on the curve $g(d)$ or its parameters. We do not pursue these in this paper.

2.2 Estimating age/depth chronologies and their uncertainty

Whatever the nature of the event, assessing the possibility of its synchroneity in two or more stratigraphic records depends upon establishing the age in each of those records. This may sometimes be done directly (although often with uncertainty) by obtaining an age estimate for material associated with the event itself; ^{14}C dating is the most common and widespread method of dating.

For some time now, Bayesian tools have been available which map radiocarbon determinations to calendar ages. Such tools do not seek to provide the user with one best calendar age. Rather they use Monte Carlo methods to generate very many calendar ages which are statistically consistent with the ^{14}C determinations. Due to fluctuations in atmospheric ^{14}C levels, radiocarbon ages must be calibrated in order to arrive at calendar age estimates. Since the calibration curve used for making this translation to the calendar scale is not monotonic (Reimer et al. 2004), the calibrated age distributions that result are typically multi-modal. Typically these are summarised for the user in the form of a density plot (usually referred to as a posterior distribution) or intervals having specified probability (e.g. 95% highest posterior density range, HDR).

Until recently the level of sophistication available for undertaking the calibration has not been matched by sophistication in the tools for constructing age-depth models. Quite a number of different methods have been used and have even been formally discussed and compared (Telford et al., 2004a,b), but only very basic attempts have been made to take into account the uncertainty on the age estimates themselves (e.g. Heegaard et al., 2005). Most use some mid-point value taken from the posterior calendar age distribution from each dated depth and use some form of interpolation to derive estimates for the ages of the non-dated depths in between (e.g. Christen and Litton, 1995). Very recent work has sought to improve on this by providing tools that take account of the uncertainty in the calibrated age estimates and, at the same time, provide estimates of the uncertainty on the interpolated age estimates too (Bronk Ramsey, 2007; Blaauw and Christen, 2005; Haslett and Parnell, 2008). In the remainder of this paper, we look in some detail at one of these (`Bchron`; Haslett and Parnell, 2008), using it to quantify the uncertainty of ages of events at selected sites.

The generic situation we consider is of one or more cores, each with samples at several known depths; their corresponding ages are unknown. A much smaller sample of depths from the same core (often overlapping with these) have been ^{14}C dated, with uncalibrated dates returned as, for example, $9680 \pm 65BP$ (mean $\pm$ 1 standard deviation), the uncertainty reflecting only the laboratory process; see Table 1 for examples.

One key feature of building chronologies is that of monotonicity; that older sediments lie beneath newer ones. Suppose for example that (a_1, a_2, a_3) are the calendar ages associated with ^{14}C dated depths (d_1, d_2, d_3). Further suppose (for simplicity of explanation) that the ages are modelled by Normal distributions with means, for example, of 5400, 5700, and 6000 years respectively and standard deviations of 200, 400 and 100 years respectively. But if we know that $d_1 < d_2 < d_3$ then we must know that $a_1 < a_2 < a_3$. A simple Monte Carlo experiment will confirm that a large sample of ages from the these distributions will contain a subset (here about 51%) of 'valid' samples. This simple ordering constraint reduces the uncertainty in a_2 from 400 years to almost 200 years. More formally the *conditional* distribution of a_2, given that $a_1 < a_2 < a_3$, has $SD = 204$ years; the conditional expected value is 5690 years, almost unchanged. Any procedure for establishing an uncertain chronology, and thus any form of interpolation to undated depths, must be built on such constraints.

2.2.1 `Bchron`

The essential idea of `Bchron` is that of stochastic linear interpolation. Under the Bayesian paradigm, we combine the interpolation with the uncertainty associated with the age determinations (such as is present in ^{14}C dates). Most importantly, `Bchron` does not produce one best chronology. Instead, it uses Monte Carlo methods to generate many complete chronologies that are consistent with the age determinations. Furthermore, `Bchron` does not exclusively require ^{14}C age determinations to construct the chronologies. More details regarding this facet of the program, as well as instructions for the installation and use of `Bchron`, are given in the appendix.

We note that the assumptions (in Bayesian terms, the prior distributions) upon which this Bayesian method is built are rather minimal; it requires only that the sedimentation history is monotone, continuous (with respect to time) and piece-wise linear; this latter can of course be used to approximate any continuous smooth curve. The method allows almost horizontal segments corresponding to periods of 'near hiatus'.

Stochastic linear interpolation in `Bchron` (discussed in more detail in Section 4, and illustrated in Figure 2) involves many repetitions of the following steps:

(1) For every dated sample, select randomly a single calendar date in a way that is consistent with the age information of all samples and with monotonicity, as discussed in the previous section.
(2) For each sample pair perform stochastic linear interpolation. This involves:
    (a) Insert a random number N of new points at random intermediate depth-age values, consistent with monotonicity.
    (b) Linearly interpolate between each of the $N + 1$ pairs.
    (c) Repeat (a) and (b) many times.
(3) Return to 1 above many times.

As described in Haslett and Parnell (2008) the underlying rationale for the above procedure is based on a model of the sedimentation process itself. This model involves a piecewise constant rate and thus a piecewise linear accumulation of sediment; the rates are positive and thus the accumulation is monotone. Both the rates and their durations are random and are such that the total accumulation in a period can be regarded as the sum of a random number N of increments each of which has a Gamma distribution. When N follows a Poisson distribution this construction is referred to as a piecewise linear Compound Poisson Gamma process. The model is flexible and leads to particularly simple implementation as above. Further, it makes minimal assumptions, for any smooth monotone curve can be thus approximated. These are in fact the features that distinguish the model from Bronk Ramsey (2007) and Blaauw and Christen (2005). Given data, Bayesian modelling permits inference on the parameters of the distributions; it thus makes very many reconstructions of the sedimentation process, all of which are equally likely and consistent with the data.

Radiocarbon-dated cores such as those we present very typically contain outliers and, in common with BCal (Buck et al., 1999) and OxCal (Bronk Ramsey, 1995, 2001), `Bchron` recognises this possibility. In an extension to previous chronology models, `Bchron` distinguishes between two different types of outlier: (1) where the calendar age probability distribution of a determination only requires a small shift to satisfy the monotonicity (older=deeper) constraint; (2) where the calendar age probability distribution requires a large shift to satisfy the monotonicity constraint. Type (1) outliers contain some useful information which can be used to inform the chronology, though a (sometimes substantial) part of their probability distribution is ignored as inconsistent with the data. Type (2) outliers are typically totally ignored and have no constraint on the chronology as constructed. The `Bchron` package reports the probability that each radiocarbon determination is an outlier of each type and uses this probability in its interpolations. Prior information can also be incorporated into the outlier detection methods. More details are provided in Haslett and Parnell (2008); examples are presented in Section 4.

Alternative proposals to `Bchron` concerning joint analysis have recently been put forward by Blaauw and Christen (2005) and by Bronk Ramsey (2007). We briefly discuss these below, but see also Haslett and Parnell (2008) for more theoretical discussion. Blaauw and Christen (2005) allow a (small) number of rate changes, corresponding to long periods of constant sedimentation. Thus several of the radiocarbon-dated points contribute to inference on the rate for each such period. However, the theoretical implications of this apparently natural way of borrowing of strength can lead to overconfidence, typically manifested in *lesser* rather than *greater* uncertainty on the ages attributable to depths which have not been radiocarbon dated. This procedure can thus severely under-estimate the uncertainties in interpolation. In our procedure the number of rate changes is conceptually larger than the number of data points (but the user does not need to specify by how much). This reflects common practice, for boundaries between very different sedimentation regimes are typically apparent and the few data points sent forward for dating are often selected from the most marked of such boundaries.

Bronk Ramsey (2007) proposes a Poisson process as an underlying monotone process on which to base an analysis. This envisages a very large number of small but instantaneous depositions of sediment; these can be referred to as 'granules'. But these depositions are conceptually of identical size, characteristic of the site under study. This gives rise to the need to estimate, by *ad hoc* methods, a fixed and unnatural 'granularity' parameter for each site. By contrast we envisage varying rates and thus smooth deposition. Furthermore such rates can vary and can be large or small; indeed small rates very naturally model the hiatus that occurs when there is very little sedimentation over a prolonged period. Bronk Ramsay's method can be thought of as an extreme and degenerate version of our procedure (see Haslett and Parnell, 2008).

2.3 Combining age and depth uncertainties

One of the great advantages of the Bayesian approach is that it is trivial to mix independent sources of uncertainty. In this context, for a given event apparent in a core (or indeed, for a series of such events), we first draw randomly from the associated depths. As discussed, the simplest model is that d_{event} is Uniform on (d_{min}, d_{max}) for each sampled d_{event}. Thus for each such depth, we interpolate stochastically, using `Bchron`. Repeating this task many times, the distribution of the sample of age values so obtained can be said to reflect both types of uncertainty.

2.4 Synchroneity

The methods outlined above allow us to sample the ages of events at different sites. Thus, to study the synchroneity of an event at two separate sites, we may repeat this procedure for both sites, forming randomly generated differences between the ages at each repetition, this generation being consistent with the data and the monotonicity. The probability distribution of such differences allows the study of synchroneity. This procedure assumes of course that the uncertainties surrounding the sedimentation histories for each core are (at least approximately) independent; we feel that this is a reasonable modelling assumption.

We repeat here our earlier claim that what we are really studying here is diachroneity. If we find that the age differences, when formed, contain very few negative (or, conversely, positive) realisations, we can strongly identify the site at which the event occurred first. Coupled to this, if the set of realisations have a small standard deviation, we can also precisely identify this age difference. In another scenario, where there are a mix of positive and negative realisations, we may not have enough evidence to determine the order. If, further, the standard deviation of the set of differences is small, we may talk about the event being 'near-synchronous'; the likely amount of time between the event occurring at different sites is well-understood and small, *these terms being capable of precise definition.*

Our general aim, in particular, is to provide a flexible approach to answering three questions about the events:

(1) In what order did the event occur at the different sites?
(2) What was the likely time difference of the occurrence of the event between sites?
(3) Is there a spatial pattern in the timing of the event?

Questions 1 and 2 are most easily answered when dealing with pairs of sites; we can use the method outlined above. When dealing with multiple sites we can use rankings (as discussed by Blackwell and Buck, 2003; Buck and Bard, 2007), which can also illustrate uncertainty in ordering.

Question 3 requires multiple sites to determine a reasonable spatial pattern. It also requires the specification of appropriate statistical measures with which to quantify such pattern; for example, rank correlation might be useful in some contexts. Basing our illustrations on only six sites, we do not pursue below a general treatment of such patterns. We remark, however, that the approach facilitates many such treatments, and we return to this in our concluding section.

Finally, we note that the questions outlined above are a small subset of those possible. Many more comparisons are available, provided that they can be formulated to give probabilities or uncertainty ranges. The software package `Bchron` provides all the necessary output files to create the ages and associated analyses in either `R` or Excel®.

3 Data used and event identification at six example sites

We illustrate the potential of this new approach by addressing the issue of the synchroneity of events as recorded in palynological data from six sites in northern Europe. The six sites selected lie along a broad west-east transect extending from the British Isles to Poland and lying between 50 and 60° N latitude (Figure 3; Table 1). In addition to requiring that sites fell along this transect, we also required: (a) that they were located below 250 m a.s.l.; (b) that their stratigraphic record spanned most of the Holocene, and at least extended from before the *Alnus* rise to after the first appearance of Cerealia-type pollen; (c) that they had a minimum of 6 radiocarbon dated samples well spread across the interval recorded; (d) that they had a sufficient number of pollen samples to provide a mean temporal resolution of *ca.* 150 years or better; and (e) that the three events we had selected for investigation were clearly recorded. The European Pollen Database (EPD) was searched for sites meeting these criteria and the required palynological and chronological data for the selected sites were downloaded (see Table 1). The six sites selected exhibit a variety of challenges to the study of synchroneity.

The three events selected for investigation were chosen because they are generally well recognised events in the Holocene vegetation history of northern Europe and are also events whose synchroneity and or causal relationships have been the subject of previous studies (see e.g. Huntley and Birks, 1983; Sturludottir and Turner, 1985; Birks, 1989; Bennett and Birks, 1990; Peglar and Birks, 1993). Each is briefly described below, paying particular attention to how the events were defined and recognised in the six sites examined. Of particular note is the fact that in some sites there was ambiguity in the stratigraphic location of an event; our approach takes account of the uncertainty in the age of the event that arises from such ambiguities. Pollen diagrams for the six sites showing the three taxa involved in the selected events are shown in Figure 4. The depths at which the events were identified in each record are shown on Figures 4 and 5 and listed in Table 1.

3.1 Alnus *rise*

For the *Alnus* rise we used the rational limit (*sensu* Smith and Pilcher, 1973) of *Alnus* pollen, defined as the first rapid increase in percentage values for the taxon. By inspection of the pollen diagrams, we identified the depth interval at each site within which d_{event} is signalled by the data. At all sites except Lilla Gloppsjön the *Alnus* rise was given a single (d_{min}, d_{max}) interval, although the apparent rapidity of the increase varied considerably between sites. This variation in apparent rate may be an artefact of differences in sampling resolution or may reflect real differences in the rate at which *Alnus* pollen abundance increased. At Lilla Gloppsjön an initial increase to moderate values was followed by a decrease before a second increase to high values; in this case both increases were used.

3.2 Ulmus *decline*

Here d_{event} is manifest as a striking decrease in relative abundance of *Ulmus* pollen, following an interval of sustained high abundance values reached after the initial increase in abundance in the early Holocene. Once again, we identified the depth interval within which d_{event} occurred by inspection of the pollen diagrams. In most sites there was a single clear *Ulmus* decline, although in two cases (Lilla Gloppsjön, Słopiec) there was more than one instance of rapid decline, a phenomenon that has been discussed by previous authors (e.g. Whittington et al., 1991).

3.3 First appearance of Cerealia-type

Here we associate d_{event} with the first mid- or late-Holocene occurrence of pollen of Cerealia-type. We identified the depth of the sample at each site in which this first occurrence was recorded. In some cases (e.g. Llyn Cororion, Słopiec) this corresponded to the empirical limit (*sensu* Smith and Pilcher, 1973), Cerealia-type pollen being present more or less continuously after its first appearance. Elsewhere, however, there were exceptionally early occurrences of single pollen grains followed by absence from many samples before a subsequent occurrence. Such isolated early occurrences may result from contamination, or may represent a pollen grain of Cerealia-type originating from a native aquatic or coastal grass (e.g *Glyceria fluitans, Elymus arenarius*), rather than indicating the early presence of a cultivated cereal. Our primary interest was in the time that elapsed between the *Ulmus* decline and the cultivation of cereals at each site. If a time lapse of zero lies in the extreme tails of the associated probability distribution we can be confident in concluding that these events are well-separated. Therefore, where such single grain occurrences substantially preceded the *Ulmus* decline, as at Wachel-3, they were ignored, whereas where they fell close to or after the *Ulmus* decline, as at Lilla Gloppsjön, alternative possible depths for the event were identified.

Having identified these three events in each record, we examine the likely temporal ordering of the sites at which each of the *Alnus* rise and *Ulmus* decline events occurred. Finally, we look at the within-core time lapse between the *Ulmus* decline and the Cerealia-type first appearance, and compare this time lapse between our different sites.

4 Results

4.1 Chronologies

Age-depth plots illustrating the chronologies obtained *via* `Bchron` for the six sites are shown in Figure 5. These plots serve to highlight a number of features of the chronologies obtained using our new technique. First, because our method develops chronologies consistent with all of the radiocarbon determinations, the age uncertainties are in some circumstances much less than those associated with individual age estimates calibrated in isolation. Thus, for example, at Lake Solso (Figure 5(d)) the availability of a large number of age estimates results in uncertainties for the age that are much less than those for individual age estimates. Similarly, at Hockham Mere (Figure 5(b)) the uncertainties in the chronology are mostly much less than the very large uncertainties of individual age estimates, especially in the early Holocene.

Second, and again because the approach develops chronologies consistent with the overall information provided by the data, some age estimates can be seen as outliers. This is generally because they are reversed relative to samples at greater depth; some are essentially ignored (see e.g. Lake Solso, Figure 5(d)). The strength of `Bchron` is that the user is not required to make an *a priori* judgement as to which age estimate(s) should be ignored; this is important because there are often no clear-cut grounds for making such judgements.

Finally, where there are large depth/time intervals between successive age estimates, the uncertainty in the chronology for samples in these intervals is often much greater than that for individual age estimates calibrated in isolation (see e.g. Llyn Cororion between *ca.* 2 and 3 m depth, Figure 5(a)). Conventional approaches to developing age-depth chronologies do not accurately reflect this additional component of uncertainty.

4.2 Event Ages

In this section we turn, in the light of the depth uncertainties identified in Section 3 and the temporal uncertainties above, to the methodologies for the study of synchroneities of events identified at certain sites. We illustrate the methods by discussing the age of the *Alnus* rise and the *Ulmus* decline. When discussing the within-core time lapse between *Ulmus* and Cerealia-type, the synchroneities are differences between cores of within-site time lapses.

In each of the following sections we discuss the answers to the three synchroneity questions from Section 2.4. For each site, we used `Bchron` to generate 10,000 plausible deposition scenarios (10 of which are shown in Table 3) and saved the resulting calendar ages for the events of interest into a file. All of our results are based on summaries of these sampled ages. We use the standard practice of presenting calibrated radiocarbon ages in calibrated years before present (cal yrs BP) using highest posterior density regions (HDRs), and rounding ages to the nearest 10 years to avoid spurious precision. We number our sites as: (1) Llyn Cororion; (2) Hockham Mere; (3) Wachel-3; (4) Lake Solso; (5) Lilla Gloppsjön; and (6) Słopiec, reflecting a West-East ordering. In the first example, the *Alnus* rise, there is a well defined and anticipated East-West pattern. This leads to a relatively straightforward set of analyses, ranging from the simple to the composite. The events associated with *Ulmus* and Cerealia-type pollen are not so simple to discuss, and these six sites do not sit well with received wisdom.

4.2.1 Alnus *rise*

Looking at the sites singly, we first see in Figure 6 (a) that the modes are well defined, at 8510, 7750, 8050, 9140, 9570 and 9890 cal yrs BP for each site respectively. These are seen to be in E-W order (as suggested by the literature) from oldest to youngest, as (6, 5, 4, 1, 3, 2), with Llyn Cororion an exception. Sites 1 (Llyn Cororion), 2 (Hockham Mere) and 4 (Lake Solso) show similar precision, with 95% intervals as in Table 4; the widths of these intervals are 440, 670, and 450 cal yrs. Sites 5 (Lilla Gloppsjön) and 6 (Słopiec) clearly show much less precision, reflected in 95% intervals widths that are more than twice as large as the first group; the long left hand tail for Słopiec is particularly to be noted. The reasons for these being so wide are rather different; at Lilla Gloppsjön it is because of the multiple depth ranges at which the *Alnus* rise is defined, whereas at Słopiec it is because of the lack of precision in the chronology at that particular depth. Several of the 95% intervals overlap, rendering statements concerning pairwise synchroneity more difficult to assert.

`Bchron` facilitates pairwise comparisons by taking age differences. For each event at each pair of sites, we take the 10,000 plausible age samples provided in the `Bchron` output and subtract one from the other to provide 10,000 samples of the length of time elapsed. With our six sites, we can thus form 15 sets of age differences, each representing a pair of sites. Figure 6 (b) presents the distribution of such differences; see also the boxed summaries in the Figure. The differences for the first pair (1 and 2; Llyn Cororion and Hockham Mere) are summarised in the top left panel. The zero point (zero age difference) is seen to lie outside the 95% interval and the density is highlighted in black; we can assert with greater than 95% probability that the *Alnus* rise occurred at Llyn Cororion before Hockham Mere. This clearly reflects the fact that the 95% intervals in Table 4 above do not overlap. But the next two panels are grey; 3 (Wachel-3) overlaps with both 1 and 2 (Llyn Cororion and Hockham Mere). Despite its long tail, 6 (Słopiec) can be clearly seen to have occurred before 2 (Hockham Mere); this cannot be said about any of the other sites. Overall, we can clearly identify the order in nine of the 15 pairs of sites.

We can take the overall discussion to a more natural overall level by computing the frequencies corresponding to different possible orderings. Thus we can consider an overall statement of E-W ordering by computing the frequency of the rank ordering (6, 5, 4, 3, 2, 1), as reflected in (a6 > a5 > a4 > a3 > a2 > a1). This is not seen in any of the ten sets of ages in Table 3; overall it occurs in just 0.02% of scenarios. We can confidently reject the statement. As the most frequent ranking of 1 (Llyn Cororion) is 3rd, this is not surprising. Is it possible that Llyn Cororion is more than an outlier, but rather a reflection of a trend more subtle than E-W? On the basis of these data, we can of course make no such statement. But it has been suggested elsewhere that genetic evidence indicates that *Alnus* in some western parts of the British Isles is more similar to populations in other western fringe areas and in southern Europe than to populations elsewhere in northern Europe, and has a different post-glacial origin and migration route from *Alnus* elsewhere in the British Isles (Hewitt, 1999). This is supported by published evidence of the early Holocene arrival of *Alnus* at other sites around the Irish Sea basin (Chambers and Price, 1985; Bennett and Birks, 1990). Thus with similar evidence from a very much larger set of sites, we can envisage an analysis based on a table of values such as in Figure 6 (a) and the computation for each row of a suitable composite statement of ordering with which to test it.

We can illustrate this further by removing Llyn Cororion from the set of sites, and computing the frequency of the age ordering (6, 5, 4, 3, 2). The scenario occurs in 38.8% of the samples. Similarly, the ordering (5, 6, 4, 3, 2) occurs in 40.2% of the samples. Part of the reason is that the dating uncertainties at (6,5) are such that 5 comes earlier than 6 about 50% of the time. The ordering ((6 or 5), 4, 3, 2) as reflected in (min(a6; a5) > a4 > a3 > a2) thus dominates the scenarios in 79.0% of samples. The next most popular ordering is (5, 4, 6, 3, 2) occurring in just 9.5% of samples.

One reason that the dating is so uncertain is the bimodality in the age for the *Alnus* decline at Lilla Gloppsjön (5), which flows directly from the fact that there are two depth candidates at this site. It can be speculated that these two depths reflect two different events, the latter of which is the Europe-wide spread of *Alnus*, the former reflecting a strictly local event. Re-running `Bchron` with only this latter depth leads to a new set of ages in the Lilla Gloppsjön column. The ordering of (6, 5, 4, 3, 2) now has a frequency of 59.6%, naturally higher than above. Of course, this provides no additional support for this theory. But it points to the fact that the attribution of two depth intervals may on occasion require the scientist to revisit the concept of 'event'. More generally, the basic methodology for evaluating composite hypotheses is seen to be simple and flexible.

The results for the *Alnus* rise are thus consistent with both strong diachroneity in the event across northern Europe and complexity in the pattern of this diachroneity. Although similar conclusions have been reached previously, our results provide for the first time realistic estimates not only of the extent of the diachroneity, but also of the uncertainty in this. They pave the way for a more extensive and systematic study of spatio-temporal pattern in this event in Holocene vegetation history across Europe more widely and using a much larger number of sites. Such an analysis would allow evaluation of inferences about the Holocene pattern of expansion of *Alnus glutinosa* across Europe made on the basis of genetic evidence (Hewitt, 1999; King and Ferris, 1998). It also would enable critical evaluation of the hypothesis that species expanded their ranges during the Holocene not principally by the advance of a continuous 'wave-like' front, but by colonising discontinuous or isolated habitat patches as they became available, perhaps as a result of some form of disturbance, subsequently 'filling-in' the landscape between the initially colonised patches (Watts, 1973).

4.2.2 Ulmus *decline*

The cause of the *Ulmus* decline has been debated in the literature (see e.g. Huntley and Birks, 1983; Edwards and Macdonald, 1991; Parker et al., 2002). Although many palaeoecologists now favour an epidemic outbreak of a 'Dutch Elm Disease' like pathogen as the most likely cause, there remains a considerable body of opinion that favours an anthropogenic cause. Whatever the cause, much literature suggests that this event was synchronous across north-western Europe; more formally, it suggests that there is no evidence that the event was diachronous.

In Figure 7 (a) (summarised in Table 4) we examine the sites singly. We see that sites 5 and 2 (Lilla Gloppsjön and Hockham Mere) are consistent with near synchroneity, having almost identical modes and 95% intervals. Conclusions for the other sites are more easily reached by pairwise comparisons; see Figure 7 (b). Seven of the 15 provide clear evidence of diachroneity, in contrast with the literature. Note that this is despite the strongly bimodal distribution at Słopiec which contributes to the uncertainty. Although near-synchroneity of the event could not be excluded for the two sites examined within the British Isles, even here the 95% range for the age difference had a width of 1370 years.

Thus, far from being more or less 'synchronous' across north-west Europe, as is often stated, the *Ulmus* decline shows considerable diachroneity. On the other hand, there is no discernible spatial pattern of diachroneity, as there was for *Alnus*. A more extensive study using many more sites is required to assess how general is the tendency for diachroneity, and also to characterise the spatial extent at which diachroneity becomes apparent. Nonetheless, if our results are confirmed then they will require new hypotheses to account for the complexity of the spatio-temporal pattern in the event. One possibility, highlighted by observations of the Dutch Elm Disease outbreak in Europe during the 1970s and 1980s, is that the pattern of occurrence and abundance of the different European *Ulmus spp.* prior to the event, and their differing susceptibility to the disease, may have influenced the spatial pattern in the timing of the event. The differing susceptibility of the *Ulmus spp.* might also account for difficulty in defining the event itself in some records if the forests around those sites supported two or more *Ulmus spp.* of differing susceptibility that may have succumbed to the disease at different times.

4.2.3 Age difference between Ulmus *decline and the appearance of Cerealia-type pollen*

It has been suggested that the *Ulmus* decline was at least accelerated by the arrival of agriculture, as evidenced by the first occurrence of Cerealia-type pollen. Such a causal relationship would be supported by apparent synchroneity of these events. The same methodology can shed light on this issue.

In this case the events being compared are recorded at the same site; i.e. the events are 'paired'. `Bchron` delivers, for each site, many chronologies (in this paper, 10,000). For each such chronology we sample pairs of ages, associated with depths from within the defined intervals for the two events, thus forming six sets of differences. The distributions of such differences are presented in Figure 8. Only at two sites, Hockham Mere and Wachel-3, was there a close temporal correspondence between the *Ulmus* decline and the first appearance of Cerealia-type pollen. The more general pattern was one in which a period of between one and four millennia elapsed after the *Ulmus* decline before Cerealia-type pollen first appeared. Although our results relate only to six sites, the hypothesis that the *Ulmus* decline generally was causally related to the spread and local establishment of cereal cultivation by Neolithic peoples has clear counter-examples in northern Europe.

Thus these six sites do not provide support for the generality of the causal hypothesis. Perhaps there was a causal relationship between the arrival of Neolithic agriculture and the elm decline at some sites but not all. No simple pattern is apparent among the six sites examined. The only obvious commonality between Hockham Mere and Wachel-3 is their relative proximity to the southern North Sea and the Rhine valley. The latter potentially might have acted as a corridor for the expansion of Neolithic peoples into the region, thus favouring the early appearance of cereal cultivation at these sites. A larger study, focussing first on the age for the first Cerealia-type pollen may well shed light on this hypothesis.

5 Discussion

We discuss the implications of the building of uncertain chronologies using `Bchron` and its use and potential in the analysis of the degree of event synchroneity.

5.1 Uncertain Chronologies

We have presented and illustrated a new method for the development of age-depth chronologies for sediment cores or other stratigraphic sequences. This new approach to modelling uncertainties in chronologies is statistically sound and robust to assumptions (Haslett and Parnell, 2008). The illustrations we present lead to a number of implications.

Joint analysis of chronologies brings a number of benefits:

- Full exploitation of the monotonicity constraints can reduce the uncertainties associated with unconstrained dated samples and can identify outliers.
- Stochastic interpolation, with appropriate and consistent statements of uncertainty, is possible for any undated depth, including depths chosen randomly within an interval. Thus depths of interest do not have to be closely bracketed by dated samples to permit study. Naturally, age uncertainty is greater for depths far from dated depths.
- Valid (if uncertain) inferences can be made about age differences for pairs of samples both within a core and between cores.
- The method is not restricted to ^{14}C dating, and can accept any source of dating information. For example, we have used the year of sampling to infer the age at the top of some of the cores.

It thus provides a platform for many types of analysis, including but not restricted to studies of event synchroneity. One important assumption underlying the method is that uncertainties in separate cores, concerning the depth-age relationship, can be treated as independent.

5.2 Methods for Studying Event Synchroneity

There are several challenges here. Not least of these is the lack of definition of the term. Nevertheless the widespread currency of terms such as 'degree of synchroneity' suggests it will survive. The approach taken here is that an event can be associated with a single depth d_{event} within a core and that the scientist can supply an interval within which this depth lies. Variations on this have no profound implications for the approach proposed here. However ,the definition of an event as an interval may have profound effects on the concept of synchroneity. Note that the use of an interval itself requires the definition of at least two precisely defined endpoints d_{start} and d_{end}. What is therefore vital is that the event be defined with respect to a specific point on a conceptual function $g(d)$ within the core. Further, difficulties of event definition must be separated from the issues of inference from noisy data.

Such variations include:

- The definition of an event as an interval in time.
- The study of events which are short-lived excursions rather than state changes.
- The specification of the uncertainty of d_{event} by models other than the Uniform distribution whose informal use has been illustrated here.

The study of indirectly observed events is typically a precursor to the study of an unobserved and typically regional space-time process. There may be more than one such process, such as the spread of agriculture and the spread of disease operating at perhaps different space-time scales. Furthermore, at least on occasion, events in a core will be local, and have no implications for regional processes. What is or is not a local event is beyond this paper. The starting point, as illustrated in Section 2, however, is the same. These are definitional issues and have no bearing on the general approach offered here. That approach is to use `Bchron` (or otherwise) to attribute ages to the 'core event(s)' which are drawn appropriately from the probability distribution of chronologies; this in turn has been fitted jointly to all the dating information that is available.

The development of full scale models for studying such space-time processes raises many other challenges. For example, elsewhere the authors use the method in palaeoclimate reconstruction (Haslett et al., 2006). Issues of the smoothness of space-time change become important. Other issues will arise in other studies.

5.3 Concluding Remarks

This new approach to obtaining age-depth chronologies and to their use in assessing synchroneity opens up new possibilities for research seeking to elucidate the spatiotemporal patterns of past ecological and environmental changes. First, by the careful use of definition and of uncertainty modelling, it may be possible to bring clarity to some debates. Second, by enabling a flexible approach to modelling uncertainty within the context of more general research, it may encourage the use of data that remain under-utilised simply because it is not clear how to handle uncertainty.

Acknowledgements

We would like to thank the authors of our six sites (R. Watkins, K.D. Bennett, W. Dörfler, B.V. Odgaard, H. Almquist-Jacobson and K. Szczepanek) for the use of their data. JH would like to thank the Durham Institute of Advanced Study. JH and AP would like thank Science Foundation Ireland for their support.

6 Appendix: Instructions for installing and using `Bchron`

`Bchron` runs as part of the free, open-source statistics package `R`. `R` can be downloaded from the website `http://lib.stat.cmu.edu/R/CRAN/` and is available for Windows, Mac OS X and Linux. The style of the program is such that, whilst simple to operate, a run of the model can take many hours due to the complex Markov chain Monte Carlo required to calibrate radiocarbon dates in a core where the dates are restricted to lie in a certain temporal order. For this reason, it is recommended to leave `Bchron` running overnight (or on a second processor) or transfer `Bchron` on to a remote workstation. In practice, the general steps required for each new core are as follows:

(1) Prepare the input files for use (see 6.4).
(2) Enter the data details via the `Bchron` menu system.
(3) For initial comparison, calibrate the radiocarbon dates without restriction.
(4) Run a `Bchron` chronology reconstruction.

(5) Predict the ages of depths in which you are interested.
(6) Produce plots of these ages or that of the entire chronology.

The software package is constantly being updated. We ask the user to contact the author if any bugs are found, or if they wish to suggest enhancements, at Andrew.Parnell@tcd.ie. The instructions below are presented for a workstation running Windows. The steps required for installation and running on other platforms are nearly identical; simply replace the `C:` with any other appropriate root directory.

6.1 Instructions for installation on a Windows machine

(1) Download and install `R` from `http://lib.stat.cmu.edu/R/CRAN/`.
(2) Download and install the packages `Bchron`, `coda` and `hdrcde` . This can be done by either downloading the packages from the link at the `R` website and choosing Packages > Install from local zip files; or via the Packages > Load Packages menu.
(3) Type `library(Bchron)` at the `R` prompt. If all has gone correctly, this should produce no error message. Typing `Bchronmenu()` should bring up the `Bchron` menu.

Once `Bchron` has been loaded correctly, some final changes are needed before it can be run;

(1) First, create a directory somewhere on the hard disk in which to store the `Bchron` files. It is recommended that this directory is `C:\Bchron` (the default assumed by `Bchron`) for ease of use.
(2) Within this directory, create three more directories called Input, Output and CalCurve.
(3) Now navigate to `C:\program files\R\R-XXX\library\Bchron\Data`, where `XXX` is the version of `R` you have installed. In here there should be a file called Rdata.zip. Alternatively, this file can be downloaded from the website: `http://www.tcd.ie/Statistics/JHpersonal/research.htm`
(4) Move the zipped files Glendalough.dat, Glendaloughddepths.txt and GlendaloughEventDepthsAlnus.txt to the input directory.
(5) Move the IntCal04.bch file to the CalCurve directory.

Everything is now set up for future runs of the program.

6.2 An example model run

An example model run using the Glendalough data:

(1) At the command prompt in `R`, type `library(Bchron)`
(2) Type `Bchronmenu()` and choose option 1.
(3) If you have followed the steps above you should not need to change the default path; you just need to tell it that the file name is Glendalough.
(4) Now choose option 2 to calibrate the radiocarbon dates.
(5) Choose option 3 to do a short run of the `Bchron` model.

Once a satisfactory short run has been obtained, a long run (return to option 3 and select a long run) should be undertaken. The long run will take much longer than the short run, but will only be required once. `Bchron` automatically provides a check for satisfactory convergence of the model run.

6.3 Example event prediction stage (with GlendaloughEventDepthsAlnus.txt)

(1) Type `Bchronmenu()` and choose Option 1.
(2) Follow step 3 as above to enter the data.
(3) Assuming a run of the `Bchron` model has already been done (as above) and that the file GlendaloughEventDepthsAlnus.txt is in the input directory, choose option 5.
(4) Check the output directory for GlendaloughEventAgesAlnusHDRs.txt which will contain 95% HDR age intervals for the depths of interest.

6.4 Input file details

Data for other cores should follow the format of the Glendalough.dat file. This example input file has 5 radiocarbon dates (and the top of the core). The columns are tab delimited and represent:

- The laboratory code of the sample.
- The radiocarbon age.
- The sample standard error.
- The depth (in cm) at which it was found.
- The thickness of the sample in cm (if the thickness is unknown, zero is acceptable).
- The outlier probabilities. The first probability identifies censored outliers as proposed by Christen (1994); the second concerns the probability a radiocarbon determination is ignored completely by the `Bchron` model. It is suggested that these two columns are left at their default values (0.05 and 0.001) for all but advanced users. Further details as to their implications can be found in Haslett and Parnell (2008).
- The data type. Choices are: a radiocarbon date (type 1), a uniformly distributed date (type 2), or a normally distributed date (type 3). For uniform

dates, the standard deviation value is taken to be the distance to the upper and lower limits. The uniform option is recommended for situations where the age at the top of the core is known with a small amount of uncertainty, or when there is dating information from an alternative source (i.e. not ^{14}C) with a known uncertainty structure. Normally-distributed (type 3) non-radiocarbon dates are allowed to be outliers, and the specified outlier probabilities are used as standard.

References

[1] Alley, R., Mayewski, P., Sowers, T., Stuiver, M., Taylor, K., Clark, P., 1997. Holocene climatic instability: A prominent, widespread event 8200 yr ago. Geology 25, 483–486.

[2] Autio, J., Hicks, S., 2004. Annual variations in pollen deposition and meteorological conditions on the fell Aakenustunturi in Northern Finland: potential for using fossil pollen as a climate proxy. Grana 43, 31–47.

[3] Bennett, K., 1983. Devensian Late Glacial And Flandrian Vegetational History At Hockham Mere, Norfolk, England. 1. Pollen Percentages And Concentrations. New Phytologist 95, 489–504.

[4] Bennett, K., Birks, H., 1990. Postglacial history of Alder (*Alnus glutinosa (L.) Gaertn.*) in the British Isles. Journal of Quaternary Science 5, 123–133.

[5] Bennett, K., Fuller, J., 2002. Determining the age of the mid-Holocene *Tsuga canadensis* (hemlock) decline, eastern North America. Holocene 12, 421–429.

[6] Birks, H., 1989. Holocene isochrone maps and patterns of tree-spreading in the British Isles. Journal of Biogeography 16, 503–540.

[7] Blaauw, M., Christen, J., 2005. Radiocarbon peat chronologies and environmental change. Journal of the Royal Statistical Society: Series C 54 (4), 805–816.

[8] Blaauw, M., Christen, J., Mauquoy, D., van der Plicht, J., Bennett, K., 2007. Testing the timing of radiocarbon-dated events between proxy archives. The Holocene 17, 283–288.

[9] Blackwell, P., Buck, C., 2003. The Late Glacial human reoccupation of north-western Europe: new approaches to space-time modelling. Antiquity 77 (296), 232–240.

[10] Boes, X., Fagel, N., 2008. Timing of the late glacial and Younger Dryas cold reversal in southern Chile varved sediments. Journal of Paleolimnology 39, 267–281.

[11] Bronk Ramsey, C., 1995. Radiocarbon calibration and analysis of stratigraphy: The OxCal program. Radiocarbon 37, 425–430.

[12] Bronk Ramsey, C., 2001. Development of the radiocarbon calibration program OxCal. Radiocarbon 43, 355–363.

[13] Bronk Ramsey, C., 2007. Deposition models for chronological records. Quaternary Science Reviews 27, 42–60.

[14] Buck, C., Bard, E., 2007. A calendar chronology for Pleistocene mammoth and horse extinction in North America based on Bayesian radiocarbon calibration. Quaternary Science Reviews 26, 2031–2035.

[15] Buck, C., Christen, J., James, G., 1999. BCal: an on-line Bayesian radiocarbon calibration tool. Internet Archaeology 7.

[16] Chambers, F., Price, S., 1985. Palaeoecology of *Alnus* (Alder): early Postglacial rise in a valley mire, North-west Wales. New Phytologist 101, 333–344.

[17] Christen, J., 1994. Summarising a set of radiocarbon determinations: a robust approach. Applied Statistics 43 (3), 489–503.

[18] Christen, J., Litton, C., 1995. A Bayesian approach to wiggle matching. Journal of Archaeological Science 22, 719–725.

[19] Davis, M., 1976. Pleistocene biogeography of temperate deciduous forests. Geoscience and Man 13, 13–26.

[20] Davis, M., 1983. Holocene vegetational history of the eastern United States. In: Wright Jr, H. (Ed.), Late Quaternary Environments of the United States, 2. The Holocene. University of Minnesota Press, pp. 166–181.

[21] Dörfler, W., 1989. Pollenanalytische Untersuchungen zur Vegetations- und Siedlungsgeschichte im Sden des Landkreises Cuxhaven, Niedersachsen. Probleme der Kstenforschung im sdlichen Nordseegebiet 17, 1–75.

[22] Edwards, K., Macdonald, G., 1991. Holocene Palynology. 2. Human influence and vegetation change. Progress in Physical Geography 15, 364–391.

[23] Haas, J., Richoz, I., Tinner, W., Wick, L., 1998. Synchronous Holocene climatic oscillations recorded on the Swiss Plateau and at timberline in the Alps. Holocene 8, 301–309.

[24] Haslett, J., Parnell, A., 2008. A simple monotone process with application to radiocarbon dated depth chronologies. Journal of the Royal Statistical Society: Series C 57 (5), 1–20.

[25] Haslett, J., Whiley, M., Bhattacharya, S., Mitchell, F., Allen, J., Huntley, B., Wilson, S., Salter-Townshend, M., 2006. Bayesian palaeoclimate reconstruction. Journal of the Royal Statistical Society, Series A 169 (3), 395–438.

[26] Heegaard, E., Birks, H., Telford, R., 2005. Relationships between calibrated ages and depth in stratigraphical sequences: an estimation procedure by mixed-effect regression. The Holocene 15, 612–618.

[27] Hewitt, G., 1999. Post-glacial re-colonization of European biota. Biological Journal of the Linnean Society 68, 87–112.

[28] Huntley, B., Birks, H., 1983. An atlas of past and present pollen maps for Europe: 0-13000 B.P. Cambridge University Press.

[29] King, R., Ferris, C., 1998. Chloroplast DNA phylogeography of *Alnus glutinosa (L.) Gaertn.* Molecular Ecology 178, 1151–1161.

[30] McColl, L. J., 2008. Statistical tools for investigating contemporaneity and co-location in archaeological records. Ph.D. thesis, University of Sheffield, Sheffield, UK.

[31] Odgaard, B., 1988. Heathland history in western Jutland Denmark. In: Birks, H. (Ed.), The cultural landscape. Past, present and future. Cambridge University Press, pp. 309–319.

[32] Parker, A., Goudie, A., Anderson, D., Robinson, M., Bonsall, C., 2002. A review of the mid-Holocene elm decline in the British Isles. Progress in Physical Geography 26, 1–45.

[33] Peglar, S., Birks, H., 1993. The mid-Holocene *Ulmus* fall at Diss Mere, South-East England : disease and human impact? Vegetation History and Archaeobotany 2, 61–68.

[34] Reimer, P. J., Baillie, M. G., Bard, E., Bayliss, A., Beck, W. W., Bertrand, C. J., Blackwell, P. G., Buck, C. E., Burr, G. S., Cutler, K. B., Damon, P. E., Edwards, L. L., Fairbanks, R. G., Friedrich, M., Guilderson, T. P., Hogg, A. G., Hughen, K. A., Kromer, B., Mccormac, G., Manning, S., Ramsey, C. B., Reimer, R. W., Remmele, S., Southon, J. R., Stuiver, M., Talamo, S., Taylor, F., van der Plicht, J. v. d., Weyhenmeyer, C. E., 2004. Intcal04 terrestrial radiocarbon age calibration, 0-26 cal kyr bp. Radiocarbon 46 (3), 1029–1058.

[35] Smith, A., Pilcher, J., 1973. Radiocarbon dates and vegetational history of the British Isles. New Phytologist 72 (4), 903–914.

[36] Sturludottir, S., Turner, J., 1985. The elm decline at Pawlaw Mire: an anthropogenic interpretation. New Phytologist 99, 323–329.

[37] Szczepanek, K., 1992. The peat-bog at Słopiec and the history of the vegetation of the Gory Swietokrzyskie Mountains (Central Poland) in the past 10,000 years. Veroff. Geobot. Inst. ETH, Stiftung Rnbel, Znrich 107, 365–368.

[38] Telford, R., Heegaard, E., Birks, H., 2004a. The intercept is a poor estimate of a calibrated radiocarbon age. Holocene 14, 296–298.

[39] Telford, R., Heegaard, E., Birks, H., 2004b. All age-depth models are wrong: but how badly? Quaternary Science Reviews 23, 1–5.

[40] Turney, C., Roberts, R., de Jonge, N., Prior, C., Wilmshurst, J., McGlone, M., Cooper, J., 2007. Redating the advance of the New Zealand Franz Josef Glacier during the Last Termination: evidence for asynchronous climate change. Quaternary Science Reviews 26, 3037–3042.

[41] Watkins, R., Scourse, J. D., Allen, J. R. M., 2007. The Holocene vegetation history of the Arfon Platform, North Wales, UK. Boreas 36, 170–181.

[42] Watts, W., 1973. Rates of change and stability in vegetation in the perspective of long periods of time. In: Birks, H., West, R. (Eds.), Quaternary plant ecology. Blackwell Scientific Publications, pp. 195–206.

[43] Whittington, G., Edwards, K., Cundill, P., 1991. Paleoecological Investigations of Multiple Elm Declines At a Site in North Fife, Scotland. Journal of Biogeography 18, 71–87.

Site name (Reference)	Latitude	Longitude	Altitude (m a.s.l.)	Number of pollen samples	Number of ^{14}C age estimates	Oldest ^{14}C age estimate	Youngest ^{14}C age estimate	Average sampling resolution (cm/sample)
Llyn Cororion (Watkins et al., 2007)	53.200°N	4.000°W	83	156	11	9680 ± 65	780 ± 60	6.1
Hockham Mere (Bennett, 1983)	52.500°N	0.833°E	33	163	23	12620 ± 85	1624 ± 45	6.5
Wachel-3 (Dörfler, 1989)	53.040°N	8.040°E	17	104	7	7320 ± 90	1120 ± 55	3.2
Lake Solso (Odgaard, 1988)	58.133°N	8.633°E	41	66	34	9180 ± 130	1680 ± 55	7.5
Lilla Gloppsjön (Almquist-Jacobson, unpub. data)	59.800°N	14.630°E	198	86	11	9560 ± 100	1840 ± 60	4.0
Słopiec (Szczepanek, 1992)	50.783°N	20.783°E	248	68	11	10280 ± 210	<120	7.5

Table 1
Details of sites used

Site name	Depth of *Alnus* rise (cm)	Depth of *Ulmus* decline (cm)	Depth of first Cerealia-type occurrence (cm)
Llyn Cororion	702-696	384-376	240
Hockham Mere	500-484	364-344	348
Wachel-3	297-293	235-233	231
Lake Solso	540-536	478-476	308
Lilla Gloppsjön	2888-2884 or 2876-2872	2772-2764 or 2760-2756	2648 or 2588
Słopiec	345-335	245-240 or 215-205	155

Table 2
Identified depths

Llyn Cororion	Hockham Mere	Wachel-3	Lake Solso	Lilla Gloppsjön	Słopiec
8524	7804	8179	9070	10229	9730
8421	7517	8292	9195	9658	9350
8484	7835	7953	9239	10190	9884
8536	7896	8085	9153	9974	10044
8543	7654	8137	9278	9965	96602
8398	7901	7906	9212	10341	9952
8596	7730	7787	8903	10622	9900
8499	7887	8318	9236	9926	9965
8552	7661	8169	9075	9674	9795
8589	7735	7994	9265	9637	10045

Table 3
Set of 10 sample ages (cal yrs BP) for the *Alnus* rise at the different sites. Taken from a much larger set of 10,000 sampled ages, and used to determine the probability distributions for the ages, and then their associated synchroneity.

	95% probability age ranges (cal yrs)		
Site name	*Alnus* rise (cal BP)	*Ulmus* decline (cal BP)	Time lapse between *Ulmus* decline and Cerealia-type
Llyn Cororion	8,240 to 8,680	5,590 to 6,050	1,270 to 3,890
Hockham Mere	7,270 to 7,940	4,860 to 6,080	-560 to 940
Wachel-3	7,420 to 8,450	4,170 to 5,250	-530 to 970
Lake Solso	8,900 to 9,350	5,480 to 6,600	2,760 to 3,900
Lilla Gloppsjön	9,330 to 10,530	4,860 to 5,670	2,260 to 3,200
Słopiec	8,170 to 10,440	2,890 to 4,800	880 to 3,410

Table 4
95% highest posterior density regions for different events of interest at each site.

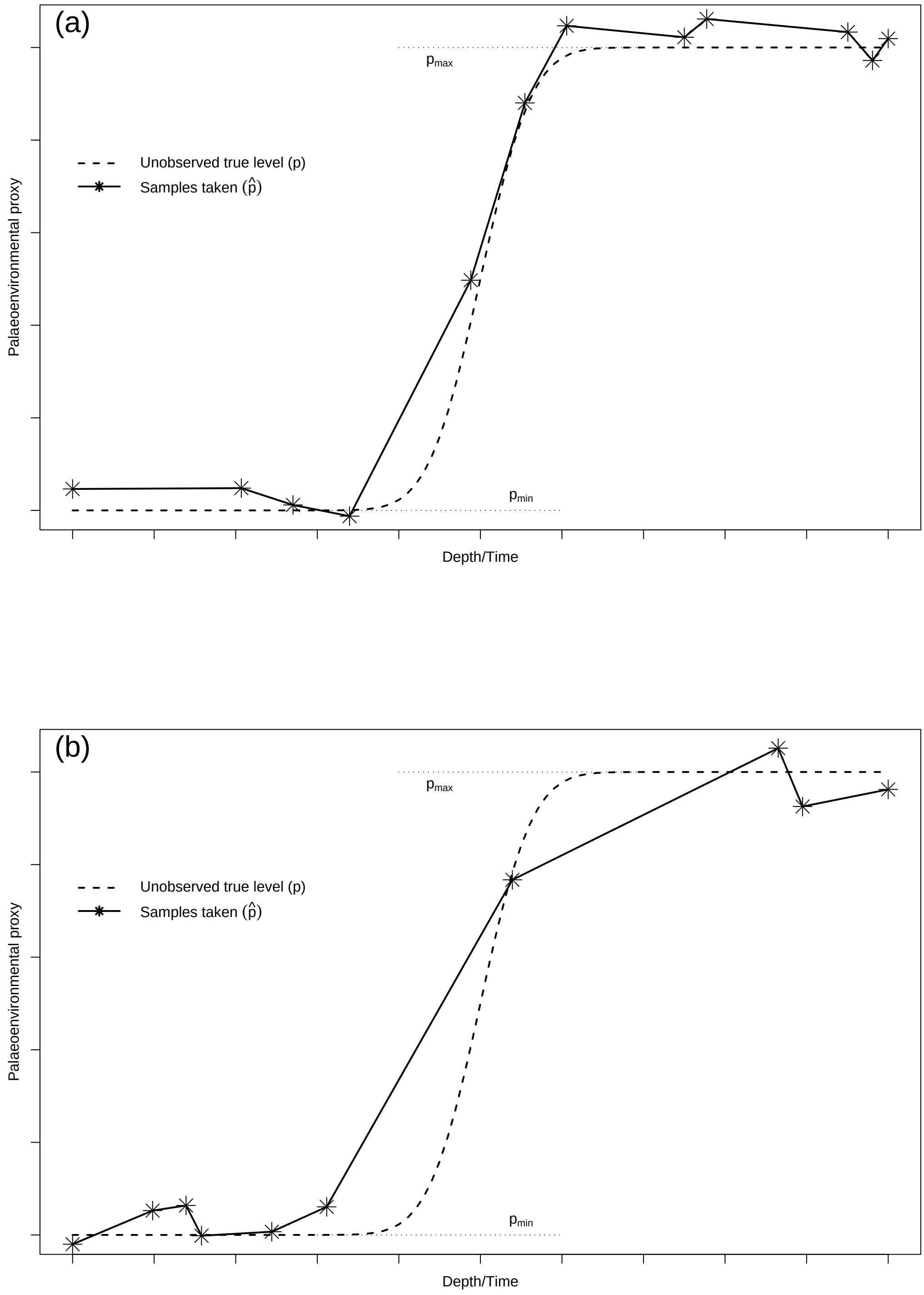

Fig. 1. Events in stratigraphic sequences. Panels illustrate how events are typically represented by the samples taken at intervals in stratigraphic sequences (stars represent samples). The unobserved true level (p) rises from a minimum (p_{min}) to a maximum (p_{max}). The contrast in sampling between panels (a) and (b) show the difficulties in identifying the location of an event.

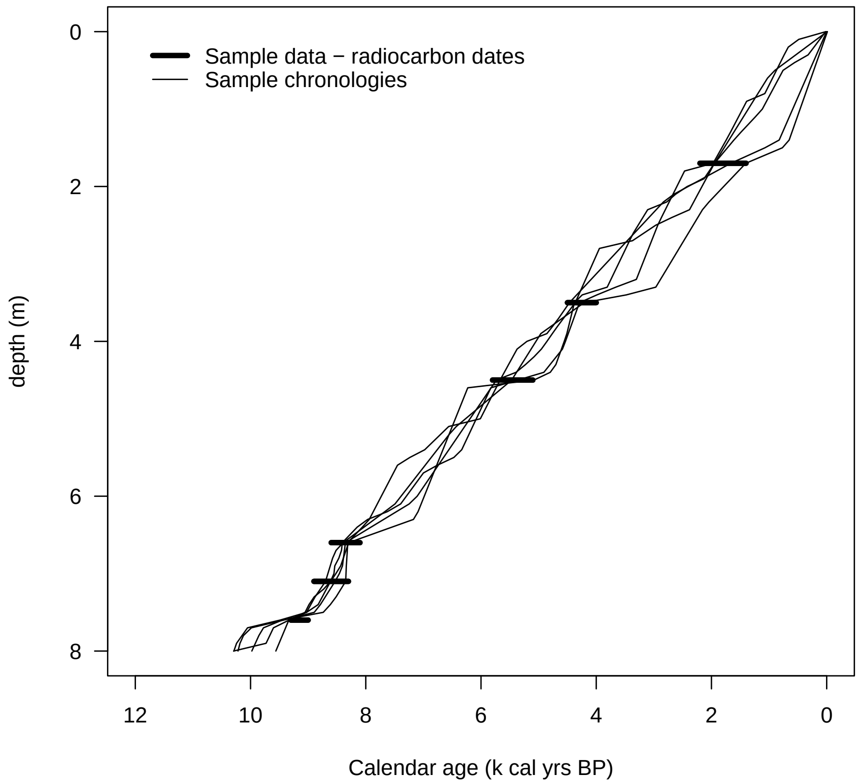

Fig. 2. Plot of `Bchron` example chronologies. The graph shows 5 stochastically interpolated chronologies sampled to fit radiocarbon data. Taken from Haslett and Parnell (2008)

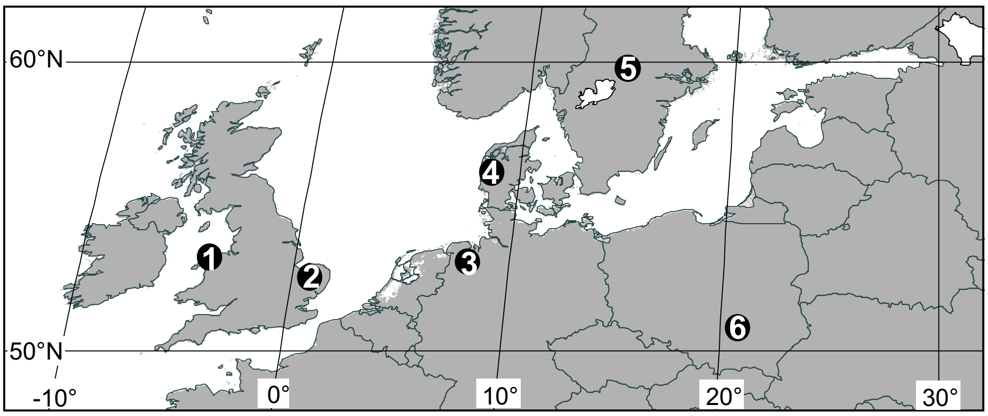

Fig. 3. Map of sites used: 1 – Llyn Cororion, 2 – Hockham Mere, 3 – Wachel-3, 4 – Lake Solso, 5 – Lilla Gloppsjön, 6 – Słopiec.

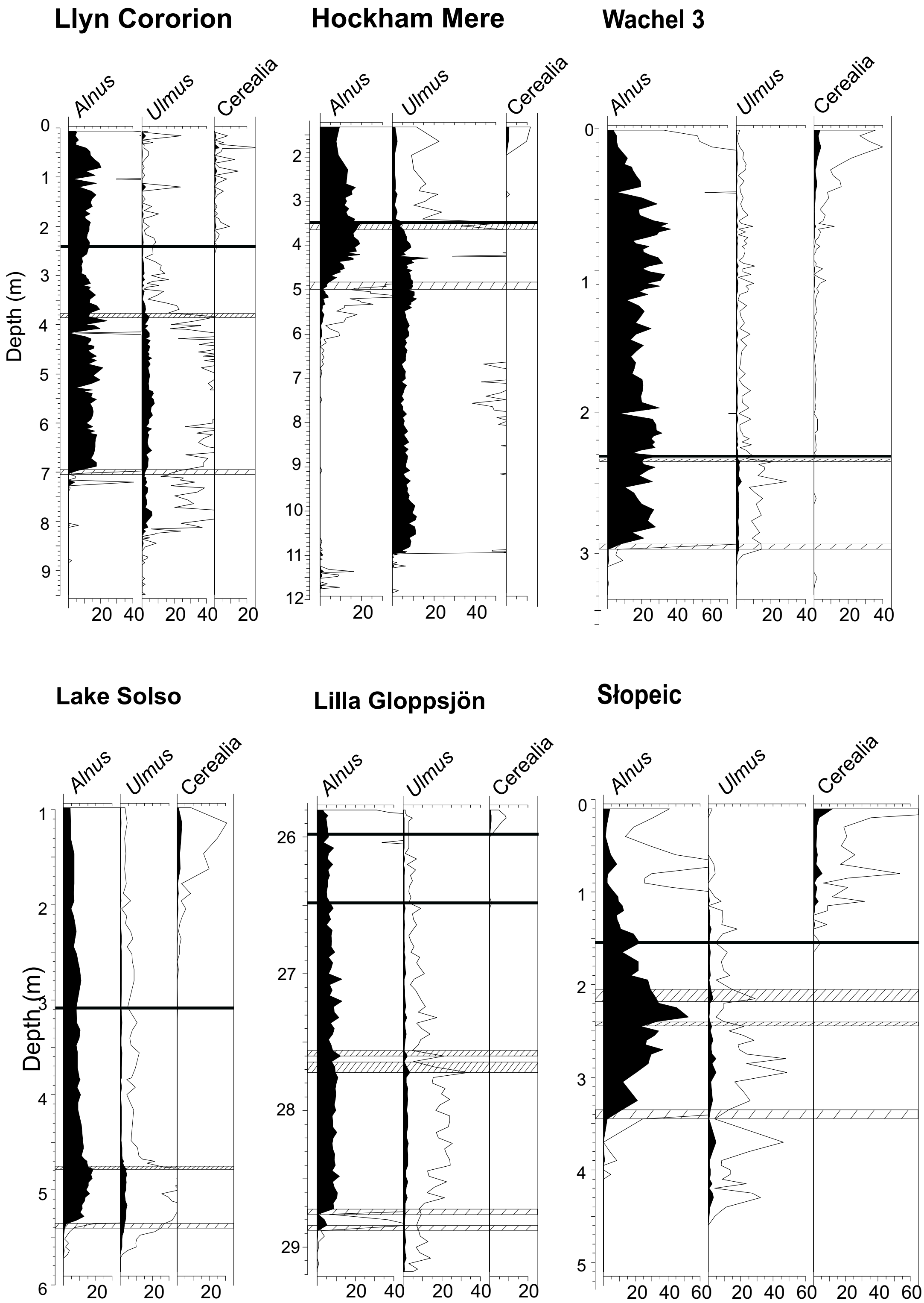

Fig. 4. Pollen percentage diagrams for the six sites showing only the selected taxa (Percentage calculation sum = Σ total land pollen). Horizontal lines indicate the possible depths of the events (light density: *Alnus* rise; higher density: *Ulmus* decline; black: First occurrence of Cerealia-type close to the *Ulmus* decline.

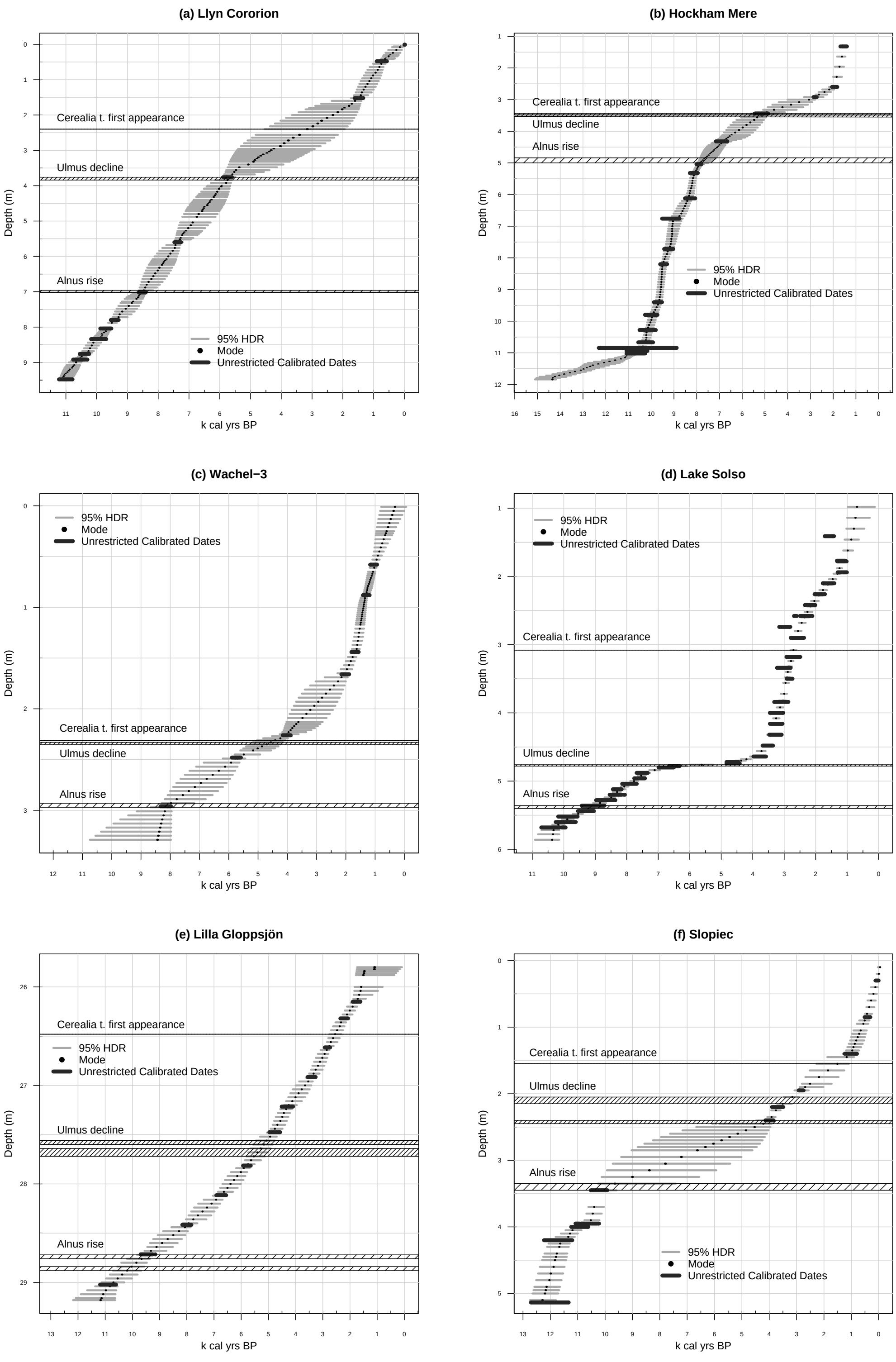

Fig. 5. Calendar year chronologies for the six sites constructed using `Bchron`. The 95% highest density regions (HDR) indicate the uncertainty of the ages assigned to the samples between the dated depths, together with the modal age for each sample. The thick black lines represent the calibrated radiocarbon ages, if the determinations had been used individually. The horizonal lines indicate the events identified in Figure 4.

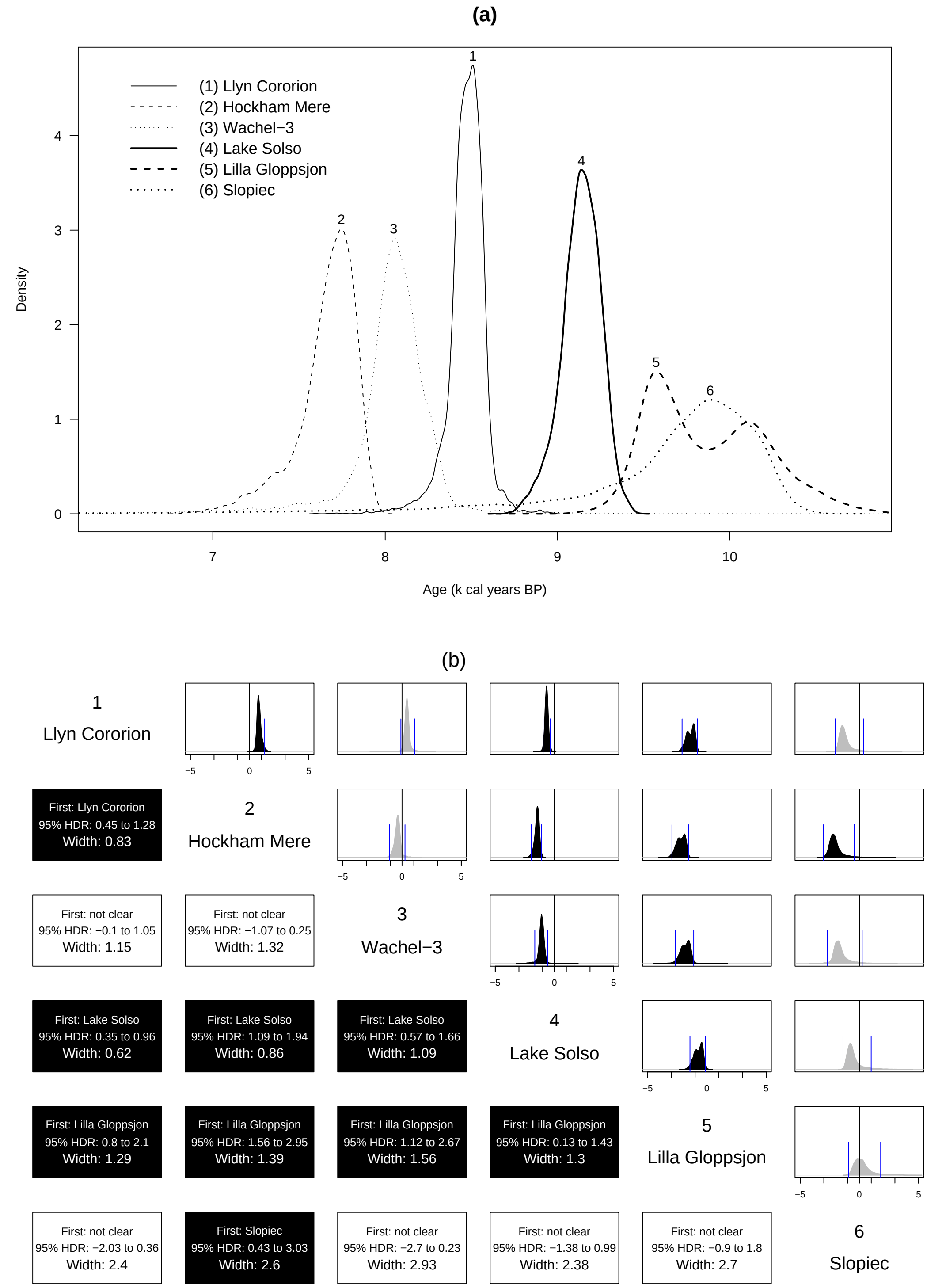

Fig. 6. (a) Probability distributions for the age of the *Alnus* rise at the six sites. (b) Pairwise synchroneity of *Alnus* rise (k cal years). The upper triangle shows the probability distribution for the estimated age difference between pairs of cores. Black distributions are given where there is strong evidence of ordering, grey where there is little or no evidence. The shorter vertical lines give the 95% HDRs. The lower triangle represents this information in text format.

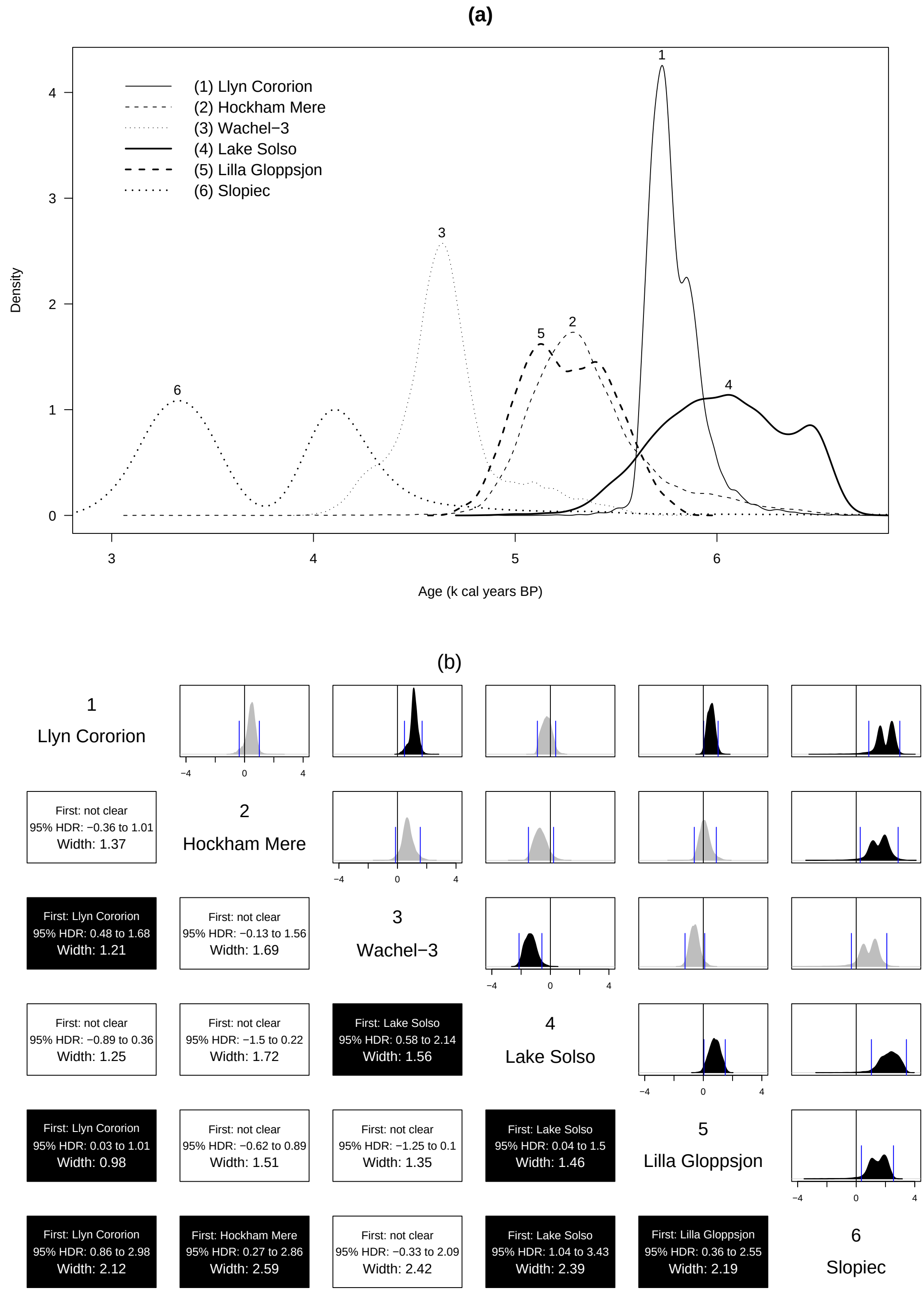

Fig. 7. (a) Probability distributions for the age of the *Ulmus* decline at the six sites. (b) Pairwise synchroneity of *Ulmus* decline (k cal years). The upper triangle shows the probability distribution for the estimated age difference between pairs of cores. Black distributions are given where there is strong evidence of ordering, grey where there is little or no evidence. The shorter vertical lines give the 95% HDRs. The lower triangle represents this information in text format.

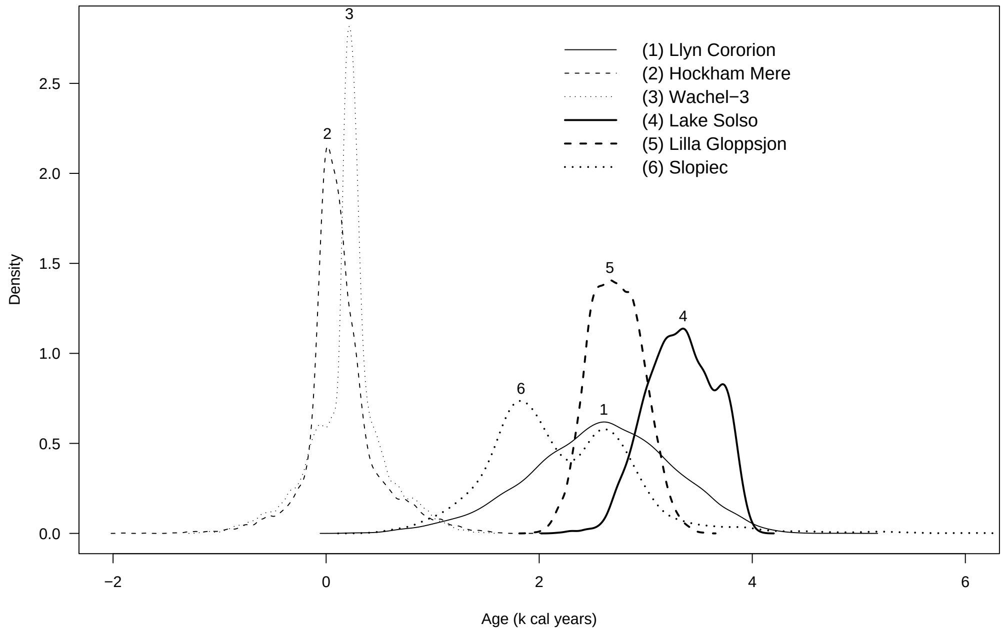

Fig. 8. Probability distributions for the time lapse between the *Ulmus* decline and the first appearance of Cerealia-type at the six sites.